

Article

Further Characterization of the BB Zircon via SIMS and MC-ICP-MS for Li, O, and Hf Isotopic Compositions

Chao Huang^{1,2}, Hao Wang^{1,2,*}, Jin-Hui Yang^{1,2,3}, Lie-Wen Xie^{1,2,3}, Yue-Heng Yang^{1,2,3} and Shi-Tou Wu^{1,2}

¹ State Key Laboratory of Lithospheric Evolution, Institute of Geology and Geophysics, Chinese Academy of Sciences, Beijing 100029, China; huangchao@mail.iggcas.ac.cn (C.H.); jinhui@mail.iggcas.ac.cn (J.-H.Y.); xieliewen@mail.iggcas.ac.cn (L.-W.X.); yangyueheng@mail.iggcas.ac.cn (Y.-H.Y.); shitou.wu@mail.iggcas.ac.cn (S.-T.W.)

² Innovation Academy for Earth Science, Chinese Academy of Sciences, Beijing 100029, China

³ College of Earth and Planetary Sciences, University of Chinese Academy of Sciences, Beijing 100049, China

* Correspondence: wanghao@mail.iggcas.ac.cn; Tel.: +86-10-82998751

Received: 20 November 2019; Accepted: 10 December 2019; Published: 11 December 2019



Abstract: In this contribution, we report the results for the characterization of the BB zircon, a newly developed zircon reference material from Sri Lanka, via secondary ion mass spectrometry (SIMS) and multiple-collector inductively coupled plasma-mass spectrometry (MC-ICP-MS). The focus of this work was to further investigate the applicability of the BB zircon as a reference material for micro-beam analysis, including Li, O, and Hf isotopes. The SIMS analyses reveal that BB zircon is characterized by significant localized variations in Li concentration and isotopic ratio, which makes it unsuitable as a lithium isotope reference material. The SIMS-determined $\delta^{18}\text{O}$ values are $13.81\text{‰} \pm 0.39\text{‰}$ (2SD, BB16) and $13.61\text{‰} \pm 0.40\text{‰}$ (2SD, BB40), which, combined with previous studies, indicates that there is no evidence of conspicuous O isotope heterogeneity within individual BB zircon megacrysts. The mean $^{176}\text{Hf}/^{177}\text{Hf}$ ratio of BB16 determined by solution MC-ICP-MS is 0.281669 ± 0.000012 (2SD, $n = 29$) indistinguishable from results achieved by laser ablation (LA)-MC-ICP-MS. Based on the SIMS and MC-ICP-MS data, BB zircon is proposed as a reference material for the O isotope and Hf isotope determination.

Keywords: zircon; reference material; BB; Li isotopes; Hf isotopes; O isotopes; SIMS; MC-ICP-MS

1. Introduction

Micro-beam analytical techniques, including secondary ion mass spectrometry (SIMS) and laser ablation multiple-collector inductively coupled plasma-mass spectrometry (LA-MC-ICP-MS), have been increasingly used by many laboratories world-wide not only for U–Pb geochronology [1–3] but also for isotope geochemistry [4–8]. For instance, Li isotopes measured by SIMS are recognized as an important tracer in weathering processes in the crust and crustal recycling into the mantle [7,9], SIMS oxygen isotope data are applied to constrain petrogenetic conditions/mechanisms, magma sources, and any possible fluid-wall rock interactions [4,6,10], and hafnium isotopes analyzed via LA-MC-ICP-MS are considered as important tracers for magmatic processes and the evolution of global reservoirs [5,11]. Due to the inherent property of providing multi-isotopic information (e.g., U–Pb–Li–O–Hf isotope systems [10,12–14]), zircon constitutes one of the most important accessory minerals in geosciences. Thus, micro-beam isotopic analyses of zircon have increased dramatically with applications in tracing magma evolution, metamorphic reaction, and sedimentary process [1,5,7]. However, a matrix-matched reference material is necessary for accurate micro-beam isotope measurements to correct for instrument-induced mass bias and to assess external reproducibility. A number of natural zircons were identified as reference materials by previous

studies, like SL7 [15], CZ3 [16], SL13 [17], 91500 [18], Temora [19], BR266 [20], GJ-1 [21,22], Mud Tank [23], M257 [24], Plešovice [25], Sri Lanka [26], OG1/OGC [27], Penglai [28], Qinghu [29], OD-3 [30], M127 [31], BB [32,33], LGC-1 [34], GZ7/GZ8 [35], LKZ-1 [36], GHR1 [37], and SA01 [38]. However, most of them are just used as a reference material for U–Pb geochronology, and the homogeneity of Li, O, and Hf isotopic compositions was not elaborately evaluated [15,17,26,30,34,35]. Additionally, the availability of most of the natural zircon standards is limited [17,24,26,31,34–36]. Among them, BB zircon, a newly developed zircon reference material from Sri Lanka, is potentially useful because of its abundance in quantity (~300g) [33]. Previous studies have identified BB zircon as a reference material suitable for LA-ICP-MS U–Pb geochronology via LA-(MC)-ICP-MS and (chemical abrasion) isotope dilution thermal ionization mass spectrometry ((CA)-ID-TIMS), with O and Hf isotopes initially measured using SIMS and LA-(MC)-ICP-MS, respectively [32,33]. However, Li isotopes, which have great potential for revealing the incorporation of surface-derived materials into crustal magmas, have not been studied thus far. In addition, further assessment of BB zircon is required to investigate the suitability of the specimen as a reference material for calibrating in situ analyses of O and Hf isotopes via SIMS or MC-ICP-MS.

For this purpose, a further comprehensive study of the Li, O, and Hf isotopic characteristics of BB zircons is reported. We investigate its Li isotopic ratios using SIMS for the first time. In addition to extensive testing of Hf isotope composition homogeneity of BB zircon by LA-MC-ICP-MS, we determine the mean Hf isotopic ratio using the solution MC-ICP-MS method for the reliable recommended value. Furthermore, we assess its O isotope homogeneity using SIMS.

2. Sample Descriptions

Zircon megacrysts BB were collected from a placer deposit of the Ratnapura gemstone field, located in the south-western region of the Sri Lanka Highland Complex. Approximately 300 g of BB zircons, comprising some eighty grains, were acquired and numbered. Cathodoluminescence (CL) images reveal that BB zircons have no zoning or fine oscillatory zoning (Figure 1). Santos et al. [33] selected several individual crystals (e.g., BB9, BB12, BB17, BB25, and BB39) to conduct detailed U–Pb age, O, and Hf isotopic determinations via TIMS, SIMS, and LA-(MC)-ICP-MS. Additionally, U–Pb LA-MC-ICP-MS and (CA)-TIMS data of five BB zircons (BB38, BB39, BB40, BB41, and BB42) were reported by Lana et al. [32].

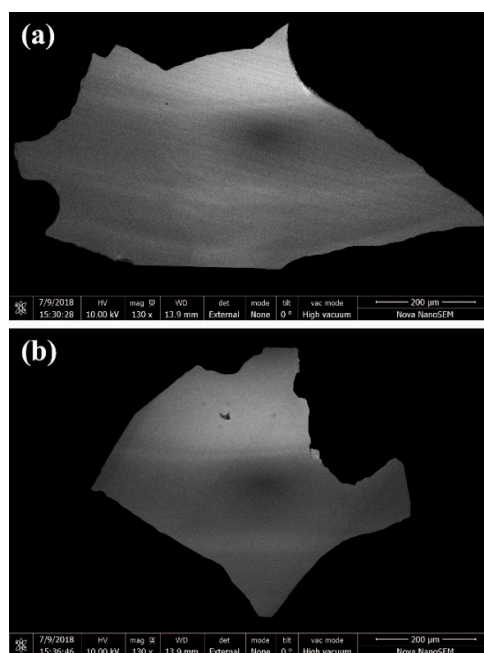


Figure 1. Cathodoluminescence (CL) images of BB16 zircon shards: (a) shard 1; (b) shard 2.

In this study, Li and O isotopes of two zircon megacrysts BB16 and BB40 were measured by SIMS, and Hf isotopic measurements were carried out using LA-MC-ICP-MS and solution MC-ICP-MS.

3. Analytical Methods

For the micro-beam analyses, one large BB40 zircon shard (~6 mm in diameter) and six BB16 zircon shards (five small (0.5–1 mm in diameter) and one large (~3 mm in diameter)) were placed in epoxy mounts together with Plešovice, Penglai, and Qinghu zircon reference materials. The shards were ground away and polished to expose their centers for analysis. In this work, the uncertainties of single analysis are stated as 2 standard errors (2SE), while the uncertainty for the grand mean value is reported as 2 standard deviations (2SD). The external reproducibility of reference materials was not propagated into the uncertainties of single measurements or final grand mean values.

3.1. SIMS Li Isotope Analysis

The Cameca IMS 1280HR ion microprobe was used for the Li isotopic measurements of BB zircons at the Institute of Geology and Geophysics, Chinese Academy of Sciences (IGGCAS) in Beijing, following the detailed procedures described by Li et al. [39]. A $20 \times 30 \mu\text{m}$ elliptical spot size was used to traverse BB zircon shards. ^6Li and ^7Li were simultaneously detected. One spot measurement comprised 60 cycles with a total measurement time of about 15 min, including pre-sputtering of 30 s, secondary beam centering of 120 s, and collection for Li isotopic signals of 720 s. Measurements of Li isotopic ratios and concentrations were corrected according to the recommended values of $\delta^7\text{Li} = 2.1\text{‰} \pm 1.0\text{‰}$ (2SD) and $[\text{Li}] = 0.86 \pm 0.18 \mu\text{g g}^{-1}$ for the M257 zircon standard.

3.2. SIMS O Isotope Analysis

The oxygen isotopic compositions of BB zircon were measured on the same Cameca IMS 1280HR ion microprobe at the IGGCAS in Beijing, with the similar analytical procedures reported by Li et al. [28] and Tang et al. [40]. The Gaussian-focused Cs^+ primary ion beam was used at 10 kv to sputter oxygen ion from BB zircon, achieving an intensity of ~1.5 nA with a spot size of about $20 \mu\text{m}$ on the sample surface. To compensate for sample charging, a normal-incidence electron gun was used. Moreover, the nuclear magnetic resonance (NMR) controller was used to stabilize the magnetic field. During the analysis, ^{16}O and ^{18}O ions were collected synchronously. The attained $^{18}\text{O}/^{16}\text{O}$ ratios were normalized to Vienna Standard Mean Ocean Water (V-SMOW, $^{18}\text{O}/^{16}\text{O} = 0.0020052$) [41]. One spot measurement involved pre-sputtering of 120 s, secondary beam centering of 120 s, and collection of oxygen isotopic signals of 60 s, with a total analytical time of about 3 min. The Penglai zircon was used as the reference material with a recommended $\delta^{18}\text{O}$ VSMOW value of $5.31\text{‰} \pm 0.10\text{‰}$ (2SD) [28]. The measurements of secondary zircon reference material Qinghu gave a grand mean $\delta^{18}\text{O}$ value of $5.37\text{‰} \pm 0.43\text{‰}$ (2SD, $n = 27$), identical to the recommended value reported in Li et al. [29]

3.3. LA-MC-ICP-MS Hf Isotope Analysis

Micro-beam Hf isotopic analyses for BB16 zircon were conducted on a Thermo Scientific Fisher Neptune Plus MC-ICP-MS coupled with a Coherent Geolas Pro 193 nm laser ablation system at the IGGCAS in Beijing (Table 1), which were similar with those reported by Wu et al. [42] and Huang et al. [43]. The LA system was operated using a beam size of $60 \mu\text{m}$ for BB and SA01 zircons and $44 \mu\text{m}$ for Mud Tank zircon with a repetition rate of 6 Hz and an energy density of $\sim 4.5 \text{ J cm}^{-2}$. Helium was used as the carrier gas with a flow rate of 640 mL min^{-1} . Aiming to achieving higher sensitivity, additional nitrogen was added to the carrier gas with a flow rate of 4 mL min^{-1} . One spot measurement comprised one block of 200 cycles with an integration time of 0.131 s. The Hf isotopic compositions of the gas blank were not measured because of the extremely low Hf signal. Correction for the isobaric interference of ^{176}Lu on ^{176}Hf was performed by measuring the intensity of the interference-free ^{175}Lu isotope ($^{176}\text{Lu}/^{175}\text{Lu} = 0.02655$) assuming $\beta_{\text{Lu}} = \beta_{\text{Yb}}$. The mean $^{173}\text{Yb}/^{172}\text{Yb}$ ratio for the individual spot analysis was used to calculate the fractionation coefficient (β_{Yb}), and the contribution of ^{176}Yb to ^{176}Hf was

corrected by applying ratios of $^{176}\text{Yb}/^{172}\text{Yb} = 0.588673$ and $^{173}\text{Yb}/^{172}\text{Yb} = 0.73925$. Instrumental mass bias was corrected based on the normalization to $^{179}\text{Hf}/^{177}\text{Hf} = 0.7325$ using the exponential law [42]. Correction for molecular interferences (e.g., $^{160}\text{Gd}^{16}\text{O}$) was not made due to low light to middle rare earth element contents in zircon. Zircon reference materials Mud Tank and SA01 analyzed during the same session gave grand mean $^{176}\text{Hf}/^{177}\text{Hf}$ values of 0.282507 ± 0.000032 (2SD, $n = 15$) and 0.282287 ± 0.000020 (2SD, $n = 15$), consistent with the reported results [23,38].

Table 1. Typical multiple-collector inductively coupled plasma-mass spectrometry (MC-ICP-MS) instrument parameters for Hf isotopic composition analysis of BB zircon.

MC-ICP-MS Cup Configuration									
Cup	L4	L3	L2	L1	C	H1	H2	H3	H4
Solution	^{173}Yb	^{175}Lu	$^{176}(\text{Lu} + \text{Hf} + \text{Yb})$	^{177}Hf	^{178}Hf	^{179}Hf	$^{180}(\text{Hf} + \text{Ta} + \text{W})$	^{181}Ta	^{183}W
Laser	^{172}Yb	^{173}Yb	^{175}Lu	^{176}Hf	^{177}Hf	^{178}Hf	^{179}Hf	^{180}Hf	^{182}W
Instrumentation									
Mass spectrometry					Thermo Fisher Neptune Plus (MC-ICP-MS)				
RF forward power					~1200 W for Laser; ~1100 W for Solution				
Interface cones					Nickel Standard Sampler cones and “H” Skimmer cones				
Sampling mode					1 block of 200 cycles for Laser; 9 blocks of 10 cycles for Solution				
Integration times					0.131 s for Laser; 4.191 s for Solution				
Background/baseline					No baseline was collected				
Carrier gas (L/min)					~0.8 for Laser; ~1 for Solution				
Laser ablation system					Geolas Pro				
Fluence					~4.5 J/cm ²				
Spot size					60 μm for BB16 and SA01; 44 μm for Mud Tank				
Ablation duration					26 s				
Sampling mode/Repetition rate					Static spot ablation/6 Hz				
Sample preparation					Conventional mineral separation, 1 inch resin mount				
Imaging					Transmissive and reflected light imaging				
Data processing									
Reference material information					Mud Tank and SA01 used as the quality control standard				
Data processing package used					For Hf isotope, an in-house Microsoft Excel macro written in VBA (Visual Basic for Applications) was used for mass fraction correction, interference correction, and uncertainty propagation				

3.4. Solution MC-ICP-MS Hf Isotope Analysis

Seven small shards (0.41–1.36 mg each) of BB16 zircon, without any pretreatment, were digested in a mixture of concentrated HNO_3 and HF using stainless steel jacketed Teflon bombs that were placed in an oven at 220 °C for three days. After evaporation, the samples were then re-dissolved in 3 mol L⁻¹ HCl. Separation and purification of the attained solutions for Lu and Hf were carried out by means of ion exchange columns using Ln Spec resin. Solution Hf isotope measurements were performed on a Thermo Fisher Scientific Neptune Plus MC-ICP-MS system at the IGGCAS in Beijing. Details of the procedure have been reported by Yang et al. [44]. Instrumental mass bias was corrected by the measured $^{179}\text{Hf}/^{177}\text{Hf}$ and its natural ratio of 0.7325. The measured ^{173}Yb and ^{175}Lu values were used to correct the possible interferences of ^{176}Yb and ^{176}Lu on ^{176}Hf , utilizing $^{176}\text{Lu}/^{175}\text{Lu} = 0.02655$ and $^{176}\text{Yb}/^{173}\text{Yb} = 0.79631$ [45]. During the solution Hf isotopic composition analysis, the Alfa Hf solution (JMC14374) was measured and yielded $^{176}\text{Hf}/^{177}\text{Hf}$ values of 0.282193 ± 0.000007 (2SD, $n = 6$) during the first session and 0.282185 ± 0.000005 (2SD, $n = 6$) during the second session, which are consistent with reported values in previous studies [42].

4. Results and Discussion

4.1. SIMS Li Isotope Composition

Twenty-one analyses were conducted on four small and one large BB16 zircon shards. The four small BB16 zircon shards have consistent $\delta^7\text{Li}$ values within analytical uncertainty and give a grand mean of $2.3 \pm 2.0\text{‰}$ (2SD). The large shard has a large $\delta^7\text{Li}$ value range from -7.5‰ to -0.6‰ . The $^7\text{Li}^+$ count rates of BB16 zircon are low and highly variable (579 to 4874 cps/nA), and the calculated Li concentrations range from 0.10 to $0.83 \mu\text{g g}^{-1}$ (Table 2 and Table S1; Figure 2a). The Li concentrations and isotopic compositions of BB40 zircon were measured along four traverses, with each traverse consisting of 19–20 analytical spots (Table 2; Figure 2b). The distance between two spots along the traverse was roughly equal, and visible cracks were avoided. Traverses 1–2 are perpendicular to traverses 3–4. The profile of Li isotopic compositions and concentrations, as revealed by traverses 1 and 2, are quite similar, namely nearly flat for the first nine analytical spots of each traverses, then rise for the subsequent 4–5 analytical spots, and finally descend for the last 5–6 analytical spots (Figure 3a,b). Although traverses 3 and 4 are parallel to each other, they give distinct trends in terms of Li isotopic compositions and concentrations. Traverse 3 shows a nearly monotonic decrease from -1.3‰ to -4.9‰ and from $1.10 \mu\text{g g}^{-1}$ to $0.78 \mu\text{g g}^{-1}$ for the $\delta^7\text{Li}$ values and Li concentrations, respectively. The $\delta^7\text{Li}$ values along traverse 4 rise dramatically from -7.1‰ to -0.6‰ and then descend to -4.4‰ , but the corresponding Li concentrations are nearly constant at about $1.0 \mu\text{g g}^{-1}$.

There are many factors that can affect the distribution of Li in zircons. Gao et al. [14] invoked the effect of diffusion to explain the phenomenon that Li contents and Li isotopic ratios are largely variable in zircon rims but homogeneous in zircon cores, which are distinct from change trends of Li contents and isotopic ratios in BB zircons. Sliwinski et al. [46] suggested that lithium in zircon is primarily sequestered within inclusions. However, transmitted light images show that no visible inclusion was detected in BB zircons. It is unclear which factors control the systemic change in Li isotopic compositions and concentrations of BB40 zircon at present. The heterogeneity of Li isotopic compositions and concentrations revealed by this study indicates that BB zircon is unusable as a reference material for micro-beam Li isotopic analysis. Several zircon reference materials used in U–Pb geochronology, including 91500, BR266, TEMORA 2, SA01, Plešovice, Penglai, and Qinghu, have been checked for the homogeneity of Li isotopic compositions, and all of them were shown to have large ranges in $\delta^7\text{Li}$ values and Li concentrations [14,38,39], which were ascribed to fast diffusion velocity of Li ion in zircon [14]. At present, only M257 and M127 have been documented to have homogenous Li isotopic compositions and concentrations [31,39]. However, these two zircon reference materials are too small in quantity to be widely used. Accordingly, it is still imperative to find more zircon reference materials with homogenous Li isotopic compositions.

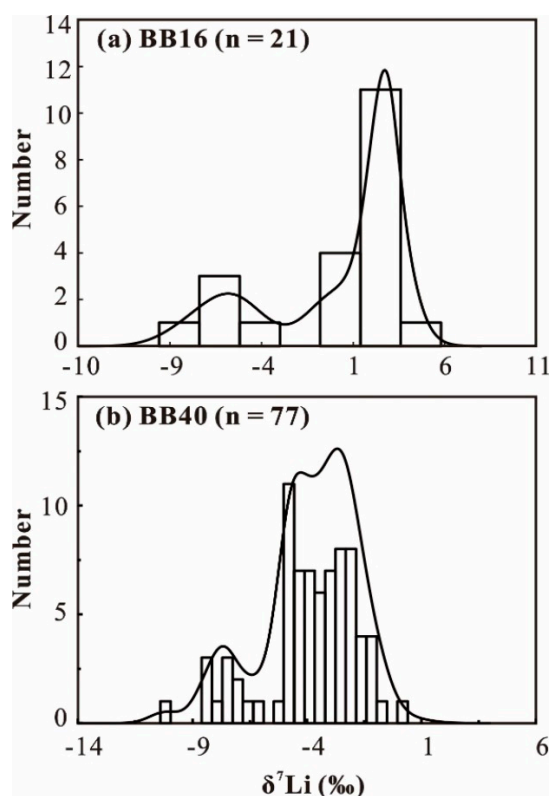


Figure 2. Histograms of measured $\delta^7\text{Li}$ values: (a) BB16 zircon; (b) BB40 zircon.

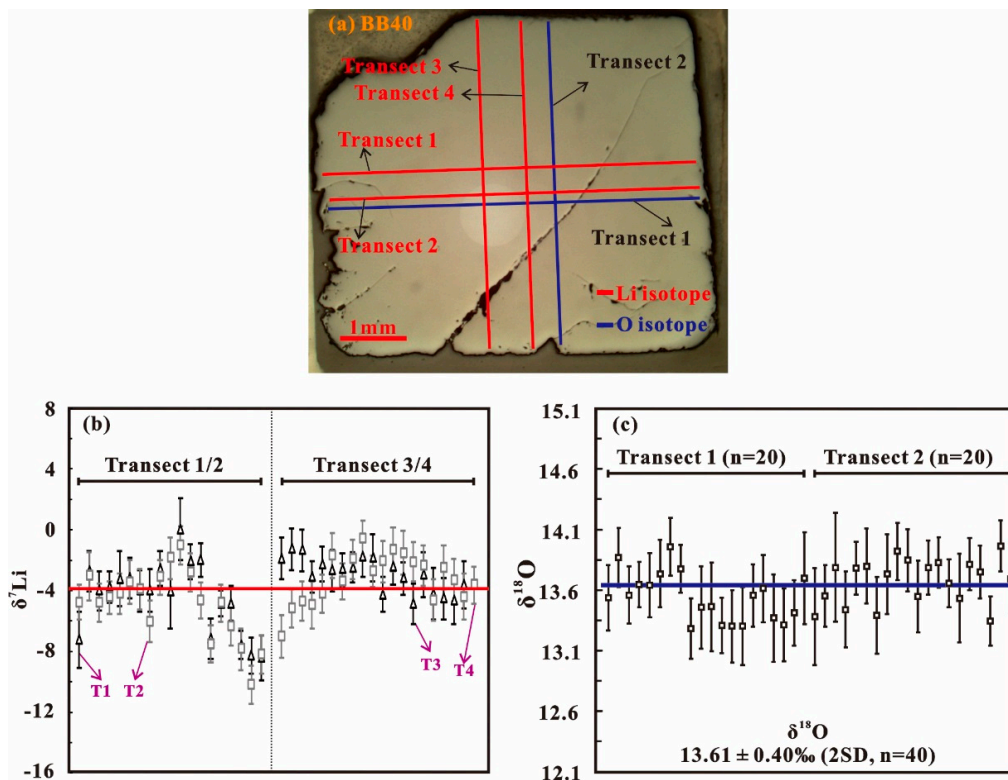


Figure 3. (a) Reflected light image of BB40 zircon; (b) profile analyses of Li isotope for BB40 zircon; (c) O isotope transecting BB40 zircon sherd. Error bars are 2SE and did not include the uncertainty of the reference material.

Table 2. Summary of Li isotopic data by secondary ion mass spectrometry (SIMS) for BB zircons.

Sample	Analysis Numbers	$\delta^7\text{Li}$ (‰) ^a				$^7\text{Li}^+$ Count Rate (cps/nA)			Li ($\mu\text{g g}^{-1}$)			
		Mean	2SD	Max	Min	Mean	Max	Min	Mean	Max	Min	
BB16	Small Shard1	5	2.6	0.6	3.0	2.2	4705	4874	4577	0.80	0.83	0.78
	Small Shard2	4	1.6	2.7	3.0	−0.1	930	1213	703	0.16	0.21	0.12
	Small Shard3	3	2.8	0.6	3.1	2.4	2785	3430	2179	0.47	0.58	0.37
	Small Shard4	3	2.3	2.2	3.7	1.1	3585	4369	2438	0.61	0.74	0.41
	Large Shard	6	−5.2	4.4	−0.6	−7.5	755	977	579	0.13	0.17	0.10
BB40	Traverse 1	19	−4.4	4.6	0	−8.5	5658	7311	3423	0.96	1.2	0.58
	Traverse 2	19	−4.9	4.5	−1	−10.2	5810	8068	3357	1.03	1.4	0.59
	Traverse 3	19	−3	2.2	−1.3	−4.9	5396	6460	4584	0.92	1.1	0.78
	Traverse 4	20	−3.2	3.2	−0.6	−7.1	5718	7115	5227	1.01	1.3	0.92

a: $\delta^7\text{Li}$ (‰) = $\delta^7\text{Li}_m - \text{IMF}$, $\delta^7\text{Li}_m = [({}^7\text{Li}/{}^6\text{Li})_m/12.039] - 1] \times 1000$; IMF = $\delta^7\text{Li}_{m(\text{M257})} - 2.1$.

4.2. SIMS O Isotope Composition

Profile analyses, comprising forty-six oxygen isotopic measurements, were conducted across six BB16 zircon shards. The $\delta^{18}\text{O}$ values determined on the six shards ($13.81\text{‰} \pm 0.27\text{‰}$ (2SD), $13.72\text{‰} \pm 0.33\text{‰}$ (2SD), $13.84\text{‰} \pm 0.42\text{‰}$ (2SD), $13.83\text{‰} \pm 0.52\text{‰}$ (2SD), $13.85\text{‰} \pm 0.32\text{‰}$ (2SD), and $13.81\text{‰} \pm 0.38\text{‰}$ (2SD)) are consistent within analytical uncertainty and form a Gaussian distribution with a grand mean of $13.81\text{‰} \pm 0.39\text{‰}$ (2SD, $n = 46$; Figure 4). Forty $\delta^{18}\text{O}$ values obtained from two profiles across the BB40 glass shard range from 13.28‰ to 13.96‰ and form a Gaussian distribution with a grand mean of $13.61\text{‰} \pm 0.40\text{‰}$ (2SD, $n = 40$; Figure 3c). No systematic trend is identified along the length of the profile.

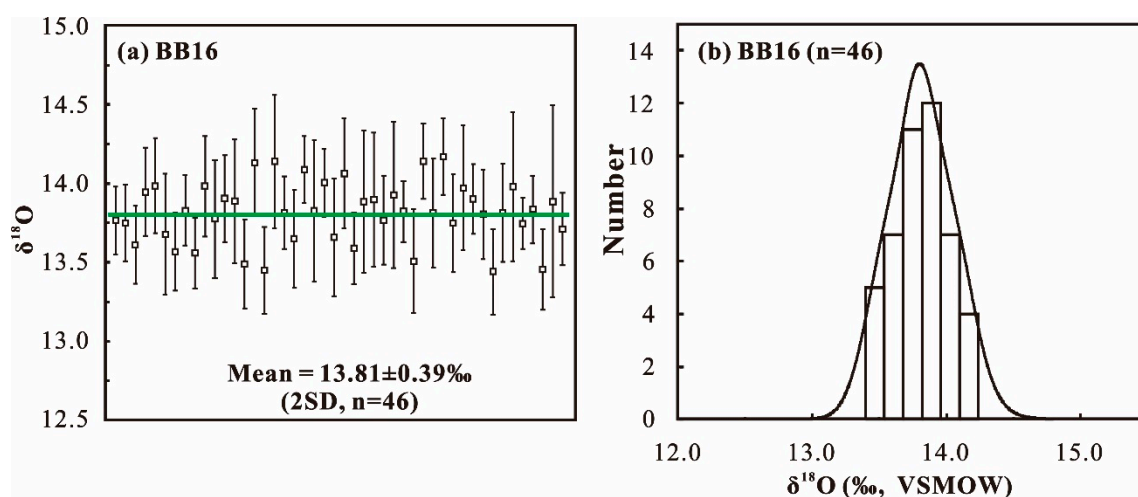


Figure 4. (a) Average of $\delta^{18}\text{O}$ values for BB16 by SIMS; (b) histogram of $\delta^{18}\text{O}$ values for BB16 by SIMS. Error bars are 2SE.

Overall, we conclude from the data set that there is no evidence of oxygen isotope heterogeneity within the BB16 and BB40 zircon crystals. BB16 and BB40 crystals have similar oxygen isotopic compositions with BB9 and BB12 within analytical uncertainty but are still about 0.8‰ to 1‰ heavier in their oxygen isotope compositions than those of the BB25 and BB39 crystals [33]. Although a systematic offset of 0.4‰ for O isotopic compositions between 91500 (the reference material used in Santos et al. [33]) and Penglai (the reference material used in this study) was detected by Santos et al. [33], this cannot explain the huge oxygen isotopic difference (1.07‰) between zircons BB16 and BB25. It is notable that BB09 zircon is 0.76‰ heavier in their oxygen isotope compositions than that of BB25 zircon, even though they were both corrected based on the recommended value of $9.86\text{‰} \pm 0.24\text{‰}$ (2SD) for 91500 [33]. All these results indicate that resolvable oxygen isotopic variations exist among different BB zircon megacrysts, as shown in Table 3 and Figure 5. In view of this, detailed and careful assessments of oxygen isotopic compositions of individual BB zircon megacrysts should be conducted before being used as oxygen reference materials. Details of SIMS oxygen isotope data are shown in Table S2.

Table 3. Summary of O isotope ratios by SIMS for BB zircons.

Reference Material	Number of Analysis	$\delta^{18}\text{O}$ (‰)	References
BB16	46	$13.81 \pm 0.39\text{‰}$ (2SD)	This study
BB40	40	$13.61 \pm 0.40\text{‰}$ (2SD)	This study
BB9	31	$13.50 \pm 0.56\text{‰}$ (2SD)	Santos et al. [33]
BB12	29	$13.43 \pm 0.32\text{‰}$ (2SD)	Santos et al. [33]
BB25	19	$12.74 \pm 0.34\text{‰}$ (2SD)	Santos et al. [33]
BB39	30	$12.83 \pm 0.20\text{‰}$ (2SD)	Santos et al. [33]

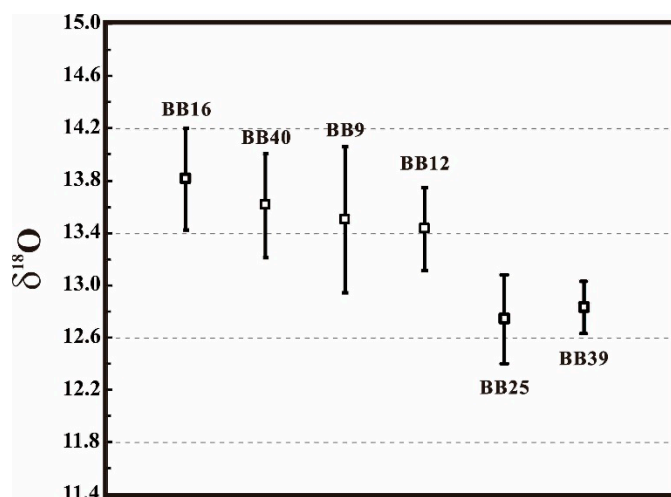


Figure 5. Averages of $\delta^{18}\text{O}$ values for BB zircons by SIMS [33]. Error bars are 2SD.

4.3. Solution and LA-MC-ICP-MS Hf Isotope Data

A total of eighty-four Hf isotope measurements by LA-MC-ICP-MS were undertaken to investigate the homogeneity of Hf isotopes on six BB16 zircon shards (Table 4). They show very low $^{176}\text{Yb}/^{177}\text{Hf}$ ratios between 0.000603 to 0.002679. There is no visible correlation between the measured $^{176}\text{Hf}/^{177}\text{Hf}$ and $^{176}\text{Yb}/^{177}\text{Hf}$ ratios (Figure 6), suggesting an accurate correction of isobaric interferences of ^{176}Yb on ^{176}Hf . Fourteen Lu–Hf isotopic analyses on BB16 zircon shard1 were conducted, and the measured $^{176}\text{Hf}/^{177}\text{Hf}$ values range from 0.281650 ± 0.000015 (2SE) to 0.281705 ± 0.000017 (2SE), with a grand mean of 0.281673 ± 0.000025 (2SD, $n = 14$). Likewise, 14 random Lu–Hf isotopic measurements were carried out on BB16 zircon shard 2, 3, 4, 5, and 6, respectively, and the results are listed in Table 4. As shown in Figure 7b,c, all the eighty-four measured $^{176}\text{Hf}/^{177}\text{Hf}$ ratios form a Gaussian distribution and give a grand mean of 0.281672 ± 0.000025 (2SD; six shards).

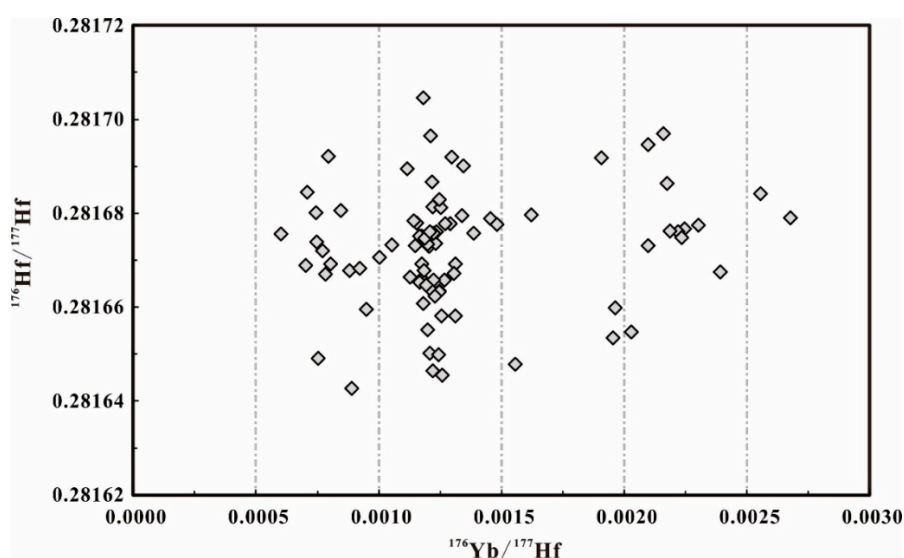


Figure 6. $^{176}\text{Hf}/^{177}\text{Hf}$ versus $^{176}\text{Yb}/^{177}\text{Hf}$ by LA-MC-ICP-MS for BB16 zircon.

Although the LA-MC-ICP-MS measurements have documented the homogeneity of Hf isotopic compositions, it is notable that no solution Hf isotope analysis has been carried out in previous studies. In this study, seven aliquots of BB16 zircons were dissolved for the chemical purification of Hf. Results of solution Hf isotope analyses by MC-ICP-MS are listed in Table 4. Twenty-nine MC-ICP-MS measurements were conducted on the seven aliquots of purified Hf solution in two sessions, which resulted in $^{176}\text{Hf}/^{177}\text{Hf}$ values of 0.281659 ± 0.000010 (2SE) to 0.281684 ± 0.000008 (2SE). In session 1, the measured $^{176}\text{Hf}/^{177}\text{Hf}$ values form a grand mean of 0.281670 ± 0.000012 (2SD, $n = 14$). Session 2 comprised fifteen measurements on the same seven aliquots of Session 1 and achieved a grand mean $^{176}\text{Hf}/^{177}\text{Hf}$ ratio of 0.281669 ± 0.000012 (2SD, $n = 15$). Overall, the grand mean for all twenty-nine solution MC-ICP-MS measurements is 0.281669 ± 0.000012 (2SD, $n = 29$; Figure 7a). The obtained $^{176}\text{Hf}/^{177}\text{Hf}$ isotopic ratios in the two sessions are identical within analytical uncertainty. Therefore, the mean $^{176}\text{Hf}/^{177}\text{Hf}$ ratio of 0.281669 ± 0.000012 (2SD) determined by solution MC-ICP-MS measurements is taken to be the best estimate of the Hf isotope compositions of BB zircon. Complete data are given in Table S3.

The results of LA-MC-ICP-MS analyses are consistent with the value of the solution MC-ICPMS results within analytical uncertainty, and indistinguishable within uncertainty from the average value of 0.281676 ± 0.000009 (2SD, $n = 16$) reported by Santos et al. [33]. Therefore, the BB16 zircon shards are fairly homogeneous in Hf isotopes at the $60 \times 60 \mu\text{m}$ sampling size and appear to lack any significant intra- and inter-shard variations. For individual analyses, see Table S3. Previous studies have also carried out many LA-MC-ICP-MS Hf isotopic measurements on other BB zircon megacrysts, and they also yielded very low $^{176}\text{Yb}/^{177}\text{Hf}$ ratios and identical $^{176}\text{Hf}/^{177}\text{Hf}$ ratios of 0.281668 ± 0.000029 (2SD) to 0.281684 ± 0.000016 (2SD) [33]. This signifies that all the BB zircon megacrysts have comparable Hf isotopic compositions. Compared to other widely-used zircon reference materials (Figure 8), BB zircons have relatively low $^{176}\text{Yb}/^{177}\text{Hf}$ ratios, and thus, they can be used as a reference material to adjust for inter-laboratory bias of the measured $^{176}\text{Hf}/^{177}\text{Hf}$ ratios, as suggested by Fisher et al. [47].

Table 4. Summary of Hf isotope data for BB zircons in this work and Santos et al. [33].

Sample No.	Method	Analysis Numbers	$^{176}\text{Yb}/^{177}\text{Hf}$	2SD	$^{176}\text{Lu}/^{177}\text{Hf}$	2SD	$^{176}\text{Hf}/^{177}\text{Hf}$	2SD
This Work								
BB16@session1	Solution	14	-	-	-	-	0.281670	0.000012
BB16@session2	Solution	15					0.281669	0.000012
BB16@shard1	LA	14	0.00121	0.00006	0.000044	0.000001	0.281673	0.000025
BB16@shard2	LA	14	0.00178	0.00117	0.000066	0.000043	0.281677	0.000027
BB16@shard3	LA	14	0.00166	0.00130	0.000060	0.000046	0.281672	0.000021
BB16@shard4	LA	14	0.00119	0.00023	0.000044	0.000008	0.281669	0.000016
BB16@shard5	LA	14	0.00097	0.00039	0.000036	0.000016	0.281669	0.000023
BB16@shard6	LA	14	0.00126	0.00013	0.000048	0.000005	0.281674	0.000031
Santos et al.								
BB1	LA	7	0.000002		0.00003		0.281670	0.000027
BB2	LA	13	0.000009		0.00015		0.281670	0.000033
BB3	LA	20	0.000004		0.00006		0.281669	0.000023
BB4	LA	5	0.000003		0.00005		0.281684	0.000016
BB5	LA	16	0.000004		0.00006		0.281669	0.000018
BB6	LA	5	0.000002		0.00004		0.281668	0.000029
BB7	LA	7	0.000002		0.00004		0.281678	0.000023
BB9	LA	20	0.000004		0.00007		0.281671	0.000012
BB10	LA	13	0.000010		0.00016		0.281677	0.000014
BB11	LA	12	0.000006		0.00010		0.281676	0.000008
BB12	LA	15	0.000009		0.00015		0.281677	0.000011
BB13	LA	12	0.000003		0.00004		0.281675	0.000009
BB14	LA	9	0.000003		0.00005		0.281678	0.000010
BB16	LA	16	0.000003		0.00005		0.281676	0.000009
BB17	LA	11	0.000003		0.00005		0.281677	0.000006
BB18	LA	16	0.000007		0.00012		0.281675	0.000010

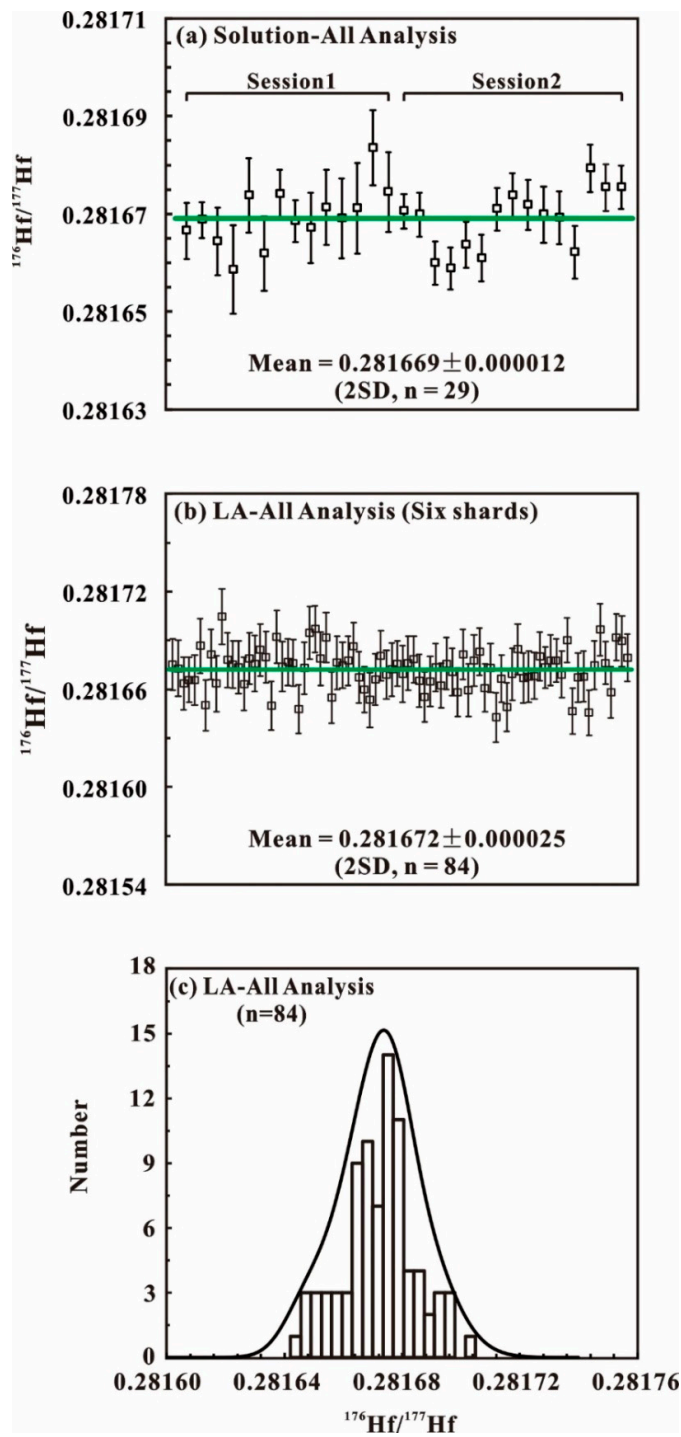


Figure 7. Averages and Histogram of $^{176}\text{Hf} / ^{177}\text{Hf}$ measurements for BB16 zircon: (a) Solution MC-ICP-MS analysis; (b,c) LA-MC-ICP-MS analysis on six BB16 zircon shards. Error bars are 2SE.

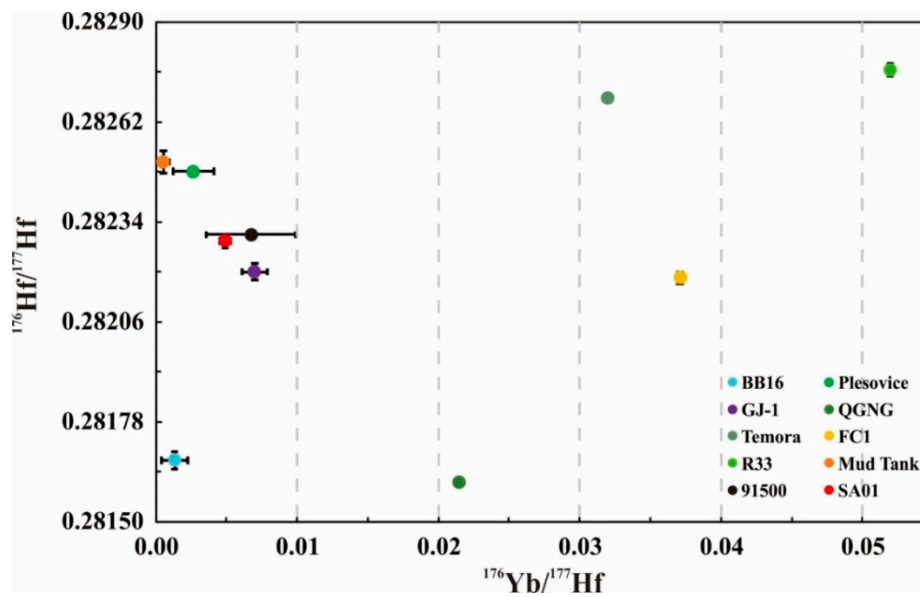


Figure 8. $^{176}\text{Hf}/^{177}\text{Hf}$ versus $^{176}\text{Yb}/^{177}\text{Hf}$ of different zircon reference materials. The data of Mud Tank, SA01, and BB16 are from this work, and the data for the other zircon reference materials are from Fisher et al. [47]. Error bars represent the range of reported $^{176}\text{Yb}/^{177}\text{Hf}$ and $^{176}\text{Hf}/^{177}\text{Hf}$ ratios in the references.

5. Conclusions

Combining our results with the earlier study by Santos et al. [33] indicates that no systematic dispersion of O isotopic compositions within single zircon megacrysts is detectable at the analytical precision of the SIMS analyses (Figures 3c and 4). However, detectable variations have been revealed among different zircon megacrysts, as shown in Table 3 and Figure 5. We strongly suggest that each BB zircon needs to be independently assessed for O isotope compositions before it can be used as a reference material.

Individual BB zircons show significant heterogeneity of Li isotopic compositions and concentrations, and thus, BB zircon cannot be used as a reference material for micro-beam Li isotopic determinations.

Beyond providing a detailed characterization via SIMS, this study conducts the testing of Hf isotope composition homogeneity of BB16 zircon by solution MC-ICP-MS. The result clearly indicates that the recommended $^{176}\text{Hf}/^{177}\text{Hf}$ value is 0.281669 ± 0.000012 (2SD), which is in good agreement with the statistical mean of LA-MC-ICP-MS analysis in this work and previous work by Santos et al. [33]. The O isotopic compositions of BB16 zircon were documented to be homogenous by SIMS analyses. Therefore, we propose that BB16 zircon is a suitable reference material for in situ Hf and O isotopic measurements of zircon.

Supplementary Materials: The following are available online at <http://www.mdpi.com/2075-163X/9/12/774/s1>, Table S1: SIMS Li isotopic data of BB zircons; Table S2: SIMS O isotopic data of BB zircons; Table S3: Solution and LA-MC-ICP-MS Hf isotopic data of BB16 zircon.

Author Contributions: Conceptualization, C.H., H.W. and J.-H.Y.; methodology, L.-W.X., Y.-H.Y., and S.-T.W.; writing—original draft preparation, C.H.; writing—review and editing, C.H., and H.W.

Funding: This research was funded by the National Key R&D Program of China (2016YFC0600109), the Natural Science Foundation of China (41525012, 41973035 and 41688103), State Key Laboratory of Lithospheric Evolution (SKL-Z201901-YT), and the Scientific Instrument Developing Project of the Chinese Academy of Sciences (YJKYYQ20170034).

Acknowledgments: We appreciate the assistance of Qiu-Li Li, Xiao-Xiao Ling, Yu Liu, Guo-Qiang Tang, Jiao Li and Hong-Xia Ma for making SIMS Li-O isotope determinations. We thank Guilherme de O. Gonçalves for kindly providing the BB16 and BB40 reference zircons.

Conflicts of Interest: The authors declare no conflict of interest. The funders had no role in the design of the study; in the collection, analyses, or interpretation of data; in the writing of the manuscript, or in the decision to publish the results.

References

1. Wang, H.; Yang, J.H.; Kroner, A.; Zhu, Y.S.; Li, R. Non-subduction origin for 3.2 Ga high-pressure metamorphic rocks in the Barberton granitoid-greenstone terrane, South Africa. *Terra Nova* **2019**, *31*, 373–380. [[CrossRef](#)]
2. Kosler, J.; Sylvester, P.J. Present trends and the future of zircon in geochronology: Laser ablation ICPMS. *Rev. Mineral. Geochem.* **2003**, *53*, 243–275. [[CrossRef](#)]
3. Ireland, T.R.; Williams, I.S. Considerations in zircon geochronology by SIMS. *Rev. Mineral. Geochem.* **2003**, *53*, 215–241. [[CrossRef](#)]
4. Zhu, Y.S.; Yang, J.H.; Sun, J.F.; Wang, H. Zircon Hf–O isotope evidence for recycled oceanic and continental crust in the sources of alkaline rocks. *Geology* **2017**, *45*, 407–410. [[CrossRef](#)]
5. Yang, J.H.; Wu, F.Y.; Wilde, S.A.; Xie, L.W.; Yang, Y.H.; Liu, X.M. Tracing magma mixing in granite genesis: In situ U–Pb dating and Hf-isotope analysis of zircons. *Contrib. Mineral. Petr.* **2007**, *153*, 177–190. [[CrossRef](#)]
6. Wang, H.; Wu, Y.B.; Yang, J.H.; Qin, Z.W.; Duan, R.C.; Zhou, L.; Yang, S.H. Crustal basement controls granitoid magmatism, and implications for generation of continental crust in subduction zones: A Sr–Nd–Hf–O isotopic study from the Paleozoic Tongbai orogen, central China. *Lithos* **2017**, *282*, 298–315. [[CrossRef](#)]
7. Ushikubo, T.; Kita, N.T.; Cavosie, A.J.; Wilde, S.A.; Rudnick, R.L.; Valley, J.W. Lithium in Jack Hills zircons: Evidence for extensive weathering of Earth’s earliest crust. *Earth Planet. Sci. Lett.* **2008**, *272*, 666–676. [[CrossRef](#)]
8. Kemp, A.I.S.; Hawkesworth, C.J.; Foster, G.L.; Paterson, B.A.; Woodhead, J.D.; Hergt, J.M.; Gray, C.M.; Whitehouse, M.J. Magmatic and crustal differentiation history of granitic rocks from Hf–O isotopes in zircon. *Science* **2007**, *315*, 980–983. [[CrossRef](#)]
9. Su, B.X.; Chen, C.; Pang, K.N.; Sakyi, P.A.; Uysal, I.; Avci, E.; Liu, X.; Zhang, P.F. Melt Penetration in Oceanic Lithosphere: Li Isotope Records from the Pozanti–Karsanti Ophiolite in Southern Turkey. *J. Petrol.* **2018**, *59*, 191–205. [[CrossRef](#)]
10. Valley, J.W. Oxygen isotopes in zircon. *Rev. Mineral. Geochem.* **2003**, *53*, 343–385. [[CrossRef](#)]
11. Bizzarro, M.; Simonetti, A.; Stevenson, R.K.; David, J. Hf isotope evidence for a hidden mantle reservoir. *Geology* **2002**, *30*, 771–774. [[CrossRef](#)]
12. Kinny, P.D.; Maas, R. Lu–Hf and Sm–Nd isotope systems in zircon. *Rev. Mineral. Geochem.* **2003**, *53*, 327–341. [[CrossRef](#)]
13. Harley, S.L.; Kelly, N.M. Zircon–Tiny but timely. *Elements* **2007**, *3*, 13–18. [[CrossRef](#)]
14. Gao, Y.Y.; Li, X.H.; Griffin, W.L.; Tang, Y.J.; Pearson, N.J.; Liu, Y.; Chu, M.F.; Li, Q.L.; Tang, G.Q.; O’Reilly, S.Y. Extreme lithium isotopic fractionation in three zircon standards (Plesovice, Qinghu and Temora). *Sci Rep.* **2015**, *5*, 16878. [[CrossRef](#)] [[PubMed](#)]
15. Kinny, P.D.; Compston, W.; Williams, I.S. A Reconnaissance Ion-Probe Study of Hafnium Isotopes in Zircons. *Geochim. Cosmochim. Acta* **1991**, *55*, 849–859. [[CrossRef](#)]
16. Pidgeon, R.T. Calibration of zircon standards for the Curtin SHRIMP II. In *Abstracts of the Eighth International Conference on Geochronology, Cosmochronology, and Isotope Geology*; Lanphere, M.A., Dalrymple, G.B., Turrin, B.D., Eds.; United States Geological Survey: Reston, VA, USA, 1994; 251p.
17. Claoué-Long, J.C.; Compston, W.; Roberts, J.; Fanning, C.M. Two carboniferous ages: A comparison of SHRIMP zircon dating with conventional zircon ages and $^{40}\text{Ar}/^{39}\text{Ar}$ analysis. In *Geochronology Time Scales and Global Stratigraphic Correlation*; Berggren, W.A., Kent, D.V., Aubrey, M.P., Hardenbol, J., Eds.; SEPM Society for Sedimentary Geology Special Publication: Tulsa, OK, USA, 1995; Volume 54, pp. 3–21. [[CrossRef](#)]
18. Wiedenbeck, M.; Alle, P.; Corfu, F.; Griffin, W.L.; Meier, M.; Oberli, F.; Vonquadt, A.; Roddick, J.C.; Spiegel, W. 3 Natural Zircon Standards for U–Th–Pb, Lu–Hf, Trace-Element and Ree Analyses. *Geostand. Newsl.* **1995**, *19*, 1–23. [[CrossRef](#)]
19. Black, L.P.; Kamo, S.L.; Allen, C.M.; Aleinikoff, J.N.; Davis, D.W.; Korsch, R.J.; Foudoulis, C. TEMORA 1: A new zircon standard for Phanerozoic U–Pb geochronology. *Chem. Geol.* **2003**, *200*, 155–170. [[CrossRef](#)]

20. Stern, R.A. A new isotopic and trace element standard for the ion microprobe: Preliminary TIMS U–Pb and electron microprobe data, current research. In *Radiogenic Age and Isotopic Studies: Report 14*; Geological Survey of Canada: Ottawa, ON, USA, 2001; 120p.
21. Jackson, S.E.; Pearson, N.J.; Griffin, W.L.; Belousova, E.A. The application of laser ablation-inductively coupled plasma-mass spectrometry to in situ U–Pb zircon geochronology. *Chem. Geol.* **2004**, *211*, 47–69. [[CrossRef](#)]
22. Morel, M.L.A.; Nebel, O.; Nebel-Jacobsen, Y.J.; Miller, J.S.; Vroon, P.Z. Hafnium isotope characterization of the GJ-1 zircon reference material by solution and laser-ablation MC-ICPMS. *Chem. Geol.* **2008**, *255*, 231–235. [[CrossRef](#)]
23. Woodhead, J.D.; Hergt, J.M. A preliminary appraisal of seven natural zircon reference materials for in situ Hf isotope determination. *Geostand. Geoanal. Res.* **2005**, *29*, 183–195. [[CrossRef](#)]
24. Nasdala, L.; Hofmeister, W.G.; Norberg, N.; Mattinson, J.M.; Corfu, F.; Dorr, W.; Kamo, S.L.; Kennedy, A.K.; Kronz, A.; Reiners, P.W.; et al. Zircon M257—A homogeneous natural reference material for the ion microprobe U–Pb analysis of zircon. *Geostand. Geoanal. Res.* **2008**, *32*, 247–265. [[CrossRef](#)]
25. Slama, J.; Kosler, J.; Condon, D.J.; Crowley, J.L.; Gerdes, A.; Hanchar, J.M.; Horstwood, M.S.A.; Morris, G.A.; Nasdala, L.; Norberg, N.; et al. Plesovice zircon—A new natural reference material for U–Pb and Hf isotopic microanalysis. *Chem. Geol.* **2008**, *249*, 1–35. [[CrossRef](#)]
26. Gehrels, G.E.; Valencia, V.A.; Ruiz, J. Enhanced precision, accuracy, efficiency, and spatial resolution of U–Pb ages by laser ablation-multicollector-inductively coupled plasma-mass spectrometry. *Geochem. Geophys. Geosy.* **2008**, *9*, Q03017. [[CrossRef](#)]
27. Stern, R.A.; Bodorkos, S.; Kamo, S.L.; Hickman, A.H.; Corfu, F. Measurement of SIMS Instrumental Mass Fractionation of Pb Isotopes During Zircon Dating. *Geostand. Geoanal. Res.* **2009**, *33*, 145–168. [[CrossRef](#)]
28. Li, X.H.; Long, W.G.; Li, Q.L.; Liu, Y.; Zheng, Y.F.; Yang, Y.H.; Chamberlain, K.R.; Wan, D.F.; Guo, C.H.; Wang, X.C.; et al. Penglai Zircon Megacrysts: A Potential New Working Reference Material for Microbeam Determination of Hf–O Isotopes and U–Pb Age. *Geostand. Geoanal. Res.* **2010**, *34*, 117–134. [[CrossRef](#)]
29. Li, X.H.; Tang, G.Q.; Gong, B.; Yang, Y.H.; Hou, K.J.; Hu, Z.C.; Li, Q.L.; Liu, Y.; Li, W.X. Qinghu zircon: A working reference for microbeam analysis of U–Pb age and Hf and O isotopes. *Chinese Sci. Bull.* **2013**, *58*, 4647–4654. [[CrossRef](#)]
30. Iwano, H.; Orihashi, Y.; Hirata, T.; Ogasawara, M.; Danhara, T.; Horie, K.; Hasebe, N.; Sueoka, S.; Tamura, A.; Hayasaka, Y.; et al. An inter-laboratory evaluation of OD-3 zircon for use as a secondary U–Pb dating standard. *Isl. Arc* **2013**, *22*, 382–394. [[CrossRef](#)]
31. Nasdala, L.; Corfu, F.; Valley, J.W.; Spicuzza, M.J.; Wu, F.Y.; Li, Q.L.; Yang, Y.H.; Fisher, C.; Muenker, C.; Kennedy, A.K.; et al. Zircon M127-A Homogeneous Reference Material for SIMS U–Pb Geochronology Combined with Hafnium, Oxygen and, Potentially, Lithium Isotope Analysis. *Geostand. Geoanal. Res.* **2016**, *40*, 457–475. [[CrossRef](#)]
32. Lana, C.; Farina, F.; Gerdes, A.; Alkmim, A.; Goncalves, G.O.; Jardim, A.C. Characterization of zircon reference materials via high precision U–Pb LA-MC-ICP-MS. *J. Anal. Atom. Spectrom.* **2017**, *32*, 2011–2023. [[CrossRef](#)]
33. Santos, M.M.; Lana, C.; Scholz, R.; Buick, I.; Schmitz, M.D.; Kamo, S.L.; Gerdes, A.; Corfu, F.; Tapster, S.; Lancaster, P.; et al. A New Appraisal of Sri Lankan BB Zircon as a Reference Material for LA-ICP-MS U–Pb Geochronology and Lu–Hf Isotope Tracing. *Geostand. Geoanal. Res.* **2017**, *41*, 335–358. [[CrossRef](#)]
34. Tian, Y.T.; Vermeesch, P.; Danisik, M.; Condon, D.J.; Chen, W.; Kohn, B.; Schwanethal, J.; Rittner, M. LGC-1: A zircon reference material for in-situ (U–Th)/He dating. *Chem. Geol.* **2017**, *454*, 80–92. [[CrossRef](#)]
35. Nasdala, L.; Corfu, F.; Schoene, B.; Tapster, S.R.; Wall, C.J.; Schmitz, M.D.; Ovtcharova, M.; Schaltegger, U.; Kennedy, A.K.; Kronz, A.; et al. GZ7 and GZ8—Two Zircon Reference Materials for SIMS U–Pb Geochronology. *Geostand. Geoanal. Res.* **2018**, *42*, 431–457. [[CrossRef](#)] [[PubMed](#)]
36. Cheong, A.C.S.; Jeong, Y.J.; Lee, S.; Yi, K.; Jo, H.J.; Lee, H.S.; Park, C.; Kim, N.K.; Li, X.H.; Kamo, S.L. LKZ-1: A New Zircon Working Standard for the In Situ Determination of U–Pb Age, O–Hf Isotopes, and Trace Element Composition. *Minerals* **2019**, *9*, 325. [[CrossRef](#)]
37. Eddy, M.P.; Ibanez-Mejia, M.; Burgess, S.D.; Coble, M.A.; Cordani, U.G.; DesOrmeau, J.; Gehrels, G.E.; Li, X.H.; MacLennan, S.; Pecha, M.; et al. GHR1 Zircon—A New Eocene Natural Reference Material for Microbeam U–Pb Geochronology and Hf Isotopic Analysis of Zircon. *Geostand. Geoanal. Res.* **2019**, *43*, 113–132. [[CrossRef](#)]

38. Huang, C.; Wang, H.; Yang, J.H.; Ramezani, J.; Yang, C.; Zhang, S.B.; Yang, Y.H.; Xia, X.P.; Feng, L.J.; Lin, J.; et al. SA01—A Proposed Zircon Reference Material for Micro-beam U–Pb Age and Hf–O Isotopic Analysis. *Geostand. Geoanal. Res.* **2020**, in press. [[CrossRef](#)]
39. Li, X.H.; Li, Q.L.; Liu, Y.; Tang, G.Q. Further characterization of M257 zircon standard: A working reference for SIMS analysis of Li isotopes. *J. Anal. Atom. Spectrom.* **2011**, *26*, 352–358. [[CrossRef](#)]
40. Tang, G.Q.; Li, X.H.; Li, Q.L.; Liu, Y.; Ling, X.X.; Yin, Q.Z. Deciphering the physical mechanism of the topography effect for oxygen isotope measurements using a Cameca IMS-1280 SIMS. *J. Anal. Atom. Spectrom.* **2015**, *30*, 950–956. [[CrossRef](#)]
41. Baertschi, P. Absolute O-18 Content of Standard Mean Ocean Water. *Earth Planet. Sci. Lett.* **1976**, *31*, 341–344. [[CrossRef](#)]
42. Wu, F.Y.; Yang, Y.H.; Xie, L.W.; Yang, J.H.; Xu, P. Hf isotopic compositions of the standard zircons and baddeleyites used in U–Pb geochronology. *Chem. Geol.* **2006**, *234*, 105–126. [[CrossRef](#)]
43. Huang, C.; Yang, Y.H.; Yang, J.H.; Xie, L.W. In situ simultaneous measurement of Rb–Sr/Sm–Nd or Sm–Nd/Lu–Hf isotopes in natural minerals using laser ablation multi-collector ICP-MS. *J. Anal. Atom. Spectrom.* **2015**, *30*, 994–1000. [[CrossRef](#)]
44. Yang, Y.H.; Zhang, H.F.; Chu, Z.Y.; Xie, L.W.; Wu, F.Y. Combined chemical separation of Lu, Hf, Rb, Sr, Sm and Nd from a single rock digest and precise and accurate isotope determinations of Lu–Hf, Rb–Sr and Sm–Nd isotope systems using Multi-Collector ICP-MS and TIMS. *Int. J. Mass. Spectrom.* **2010**, *290*, 120–126. [[CrossRef](#)]
45. Vervoort, J.D.; Patchett, P.J.; Soderlund, U.; Baker, M. Isotopic composition of Yb and the determination of Lu concentrations and Lu/Hf ratios by isotope dilution using MC-ICPMS. *Geochem Geophys Geosy* **2004**, *5*. [[CrossRef](#)]
46. Sliwinski, J.T.; Kueter, N.; Marxer, F.; Ulmer, P.; Guillong, M.; Bachmann, O. Controls on lithium concentration and diffusion in zircon. *Chem. Geol.* **2018**, *501*, 1–11. [[CrossRef](#)]
47. Fisher, C.M.; Vervoort, J.D.; Hanchar, J.M. Guidelines for reporting zircon Hf isotopic data by LA-MC-ICPMS and potential pitfalls in the interpretation of these data. *Chem. Geol.* **2014**, *363*, 125–133. [[CrossRef](#)]



© 2019 by the authors. Licensee MDPI, Basel, Switzerland. This article is an open access article distributed under the terms and conditions of the Creative Commons Attribution (CC BY) license (<http://creativecommons.org/licenses/by/4.0/>).